Analytica Chimica Acta 1082 (2019) 126–135

Contents lists available at ScienceDirect

Analytica Chimica Acta

journal homepage: www.elsevier.com/locate/aca

# Molecularly imprinted polymer SPE sensor for analysis of CA-125 on serum

Tânia S.C.R. Rebelo [a, b], Renata Costa [a], Ana T.S.C. Brandão [a], A. Fernando Silva [a], M. Goreti F. Sales [b], Carlos M. Pereira [a, *]

[a] Centro de Investigação Em Química da Universidade Do Porto, Departamento de Química e Bioquímica, Faculdade de Ciências da Universidade Do Porto, Porto, Portugal
[b] BioMark/ISEP, Instituto Superior de Engenharia Do Porto, Porto, Portugal

## HIGHLIGHTS

- MIP@AuSPE biosensor for fast CA-125 detection in point-of-care.
- Comparison between electrochemical and optical (SPR) sensor.
- MIP sensor for a low detection limit of biomolecules with high molecular weight.
- Determination of CA-125 in serum at clinically relevant levels (LOD = 0.1 U/mL).

## GRAPHICAL ABSTRACT

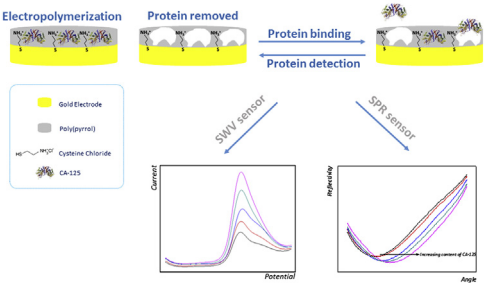


## ARTICLE INFO

*Article history:*
Received 20 March 2019
Received in revised form
29 June 2019
Accepted 22 July 2019
Available online 26 July 2019

*Keywords:*
Molecularly imprinted polymer
Carbohydrate antigen 125
SPE
SPR

## ABSTRACT

Considering the high incidence level and mortality rate of ovarian cancer, particularly among the European female population, the carbohydrate antigen 125 (CA-125) was selected as the protein target for this study for the development of a MIP-based biosensor.

This work presents the development of molecular imprinting polymers (MIPs) on gold electrode surface for CA-125 biomarker recognition. The preparation of the CA-125 imprinting was obtained by electropolymerization of pyrrole (Py) monomer in a gold electrode using cyclic voltammetry (CV) in order to obtain highly selective materials with great molecular recognition capability. The quantification of CA-125 biomarker was made through the comparison of two methods: electrochemical (square wave voltammetry -SWV) and optical transduction (surface plasmon resonance -SPR). SWV has been widely used in biological molecules analysis since it is a fast and sensitive technique. In turn, SPR is a non-destructive optical technique that provides high-quality analytical data of CA-125 biomarker interactions with MIP.

Several analytical parameters, such as sensitivity, linear response interval, and detection limit were determined to proceed to the performance evaluation of the electrochemical and optical transduction used in the development of the CA-125 biosensor.

The biosensor based in the electrochemical transduction was the one that presented the best analytical parameters, yielding a good selectivity and a detection limit (LOD) of 0.01 U/mL, providing a linear concentration range between 0.01 and 500 U/mL. This electrochemical biosensor was selected for the

* Corresponding author.
*E-mail address:* cmpereir@fc.up.pt (C.M. Pereira).

https://doi.org/10.1016/j.aca.2019.07.050

study and it was successfully applied in the CA-125 analysis in artificial serum samples with recovery rates ranging from 91 to 105% with an average relative error of 5.8%.



## 1. Introduction

At the present day, ovarian cancer is ranked as the seventh most common cancer affecting women in Europe, with an incidence level of 9.3% among all cancer diseases, presenting a 5.3% mortality rate [1]. Unfortunately, ovarian cancer is rarely diagnosed in the early stages while the tumor is still located or confined to the ovary and still easier to be treated [2]. Accurate and early detection of ovarian cancer is crucial, attributing to the early diagnosis a major role in the successful treatment of the disease.

Diagnosis and supervision of disease progression, particularly in cases of cancer, are dependent on the advance and development of new and more efficient sensors to identify the presence of biomarkers in clinical samples. Considering the high incidence level and mortality rate of ovarian cancer among the European female population, the carbohydrate antigen 125 (CA-125) was selected as the protein target for this study for the development of a MIP-based biosensor.

The carbohydrate antigen 125 (CA-125) is an important serum biomarker for ovarian cancer detection. Since Bast et al. [3] discovered it in 1981, this biomarker is approved for both monitoring treatment with chemotherapy and differential diagnosis of patients presenting a pelvic mass [4].

Early stage diagnosis of cancer is decisive for improving cancer survival besides other important clinical outcomes and its success is crucially dependent on the development of new detection techniques such as electrochemical [5–9] and optical [10–13] immunosensors for biomarker CA-125 detection.

The values of CA-125 (mucin-like glycoprotein, with a molecular mass of approximately 200 kDa [3]) in 99% of healthy donors were found to have a lower threshold of 35 U/mL [14] and in about 80% of women, the presence of higher values of CA-125 were related to the diagnosis of epithelial ovarian cancer [15]. High levels of CA-125 glycoprotein were found to be not only exclusive of epithelial ovarian cancer but also, it has been correlated with other types of cancers such as endometrial, lung, breast and gastrointestinal [16]. Although CA-125 has been clinically considered for more than 20 years as an important biomarker in diagnosing/screening purposes, for evaluating the progression of therapies and surveillance of patients with ovarian cancer, the research advances in this topic are critical in overcoming several drawbacks still existing in each domain.

Over the past years, an important breakthrough has occurred in the development of electrochemical biosensors as an alternative to conventional detection methodologies. The high selectivity of this sensors results from the immobilization of recognition elements on the sensor substrate that have a specific binding affinity to the desired molecule [5,6,9]. The recognition element can be either biological molecules or artificial materials, such as enzymes, antibodies, microorganisms, biological tissue, DNA and molecularly-imprinted polymers (MIPs) [17].

MIPs are rigid three-dimensional and synthetic materials resulted from the molecular imprinting process used in the design of sensors with selective affinity for specific targets of analytical interest such as drugs, proteins, or biomolecules through covalent or non-covalent bonds [18].

Several electrochemical detection methods of protein biomarkers based on MIPs can be found in the literature, in which proteins are covalently bonded [19] or adsorbed [20] in the surface's receptor. MIPs formation can result from chemical [19] or electrochemical [20] polymerization. Alongside with the selection of the best protein attachment to the surface and polymerization method, the careful choice of the monomer, generating polymer layers more or less conductive [21] and showing different physical features, is crucial for the success of the MIP based sensor.

A previous published article [22] regarding CA-125 detection, using MIP gold nanoelectrode ensembles and polyphenol as a monomer, showed encouraging results for practical clinic cancer diagnosis.

Polypyrrole (PPy) is an organic and conductive polymer, being first synthesized in 1912, which presents relevant and versatile functional properties as a reporting interface in electrochemical sensors. This conjugated polymer has good biocompatibility in the incorporation of biomolecules into its structure and has been the basis for the preparation of MIP-based sensors in the recognition and detection of a diversity of molecules [23]. PPy is one of the most extensively used polymers in bioanalytical sensors design and it can be electrochemically generated and deposited onto conducting surfaces [24].

Extensive research has been made focused on the PPy electropolymerization application in biosensors' electrochemical construction for the detection of several molecules [23,25–27].

Smaller, faster, cheaper and smarter biosensor diagnostic devices for molecular analysis are currently a hot topic in the developing of diagnostic technologies which is crucially dependent on innovative biosensor-based strategies [28]. As an alternative strategy to electrochemical MIP-based sensors, MIPs coupled to optical transducers (e.g. surface plasmon resonance - SPR) have become a promising tool for cancer biomarker determination. SPR based biosensors methods are the basis of many standard tools in providing highly sensitive and quality data on the study of biomolecular interactions, chemical detection and immunoassays [29,30]. SPR sensing coupled to the molecular imprinting polymerization process is considered to be one of the most suitable strategic processes to achieve highly selective polymeric materials with special molecular recognition capacity [31]. SPR sensors using MIPs were primarily developed by Lai et al. [32] for the on-site detection of theophylline, caffeine, and xanthine. Over the past years, SPR-MIP sensors have been successfully developed as a new sensing technology used to monitor biological recognition (antibodies and receptors) [33], biomolecules in clinical samples [34], environmental pollutants [35], drugs [36,37] and food safety [38,39].

This work presents the construction and compares the merits of a new CA-125 electrochemical and optical biosensor by electropolymerization on a gold screen-printed electrode (Au-SPE) and on the SPR gold sensor with monomer pyrrole (Py).

The use of Py generated highly selective printed materials for a protein and thus improve biosensor performance. CA-125 was covalently attached to the Au-SPE film, previously treated with cysteamine.

SPR is a label-free and non-destructive optical technique providing high-quality data on CA-125 MIP binding interactions in real time at a conductive interface. In this study, the several steps

involved in the molecular imprinting process, such as the template construction, the removal of the printed molecules from the polymer matrix and the rebinding of the template molecules to the polymer were followed using SPR reflectivity measurements. The detection of the CA-125 protein directly grafted on the SPR sensing chip was tracked based on the changes in the dielectric permittivity and the shift in the resonant angle of incidence of the sensor surface.

Analytical parameters such as sensitivity, selectivity, dynamic linear range and limit of detection were assessed in order to evaluate and optimize both (electrochemical and optical) CA-125 biosensor performance.

## 2. Experimental procedure

### 2.1. Synthesis of MIP on the Au-SPE

The MIP was prepared by electropolymerization of Py monomer using CA-125 as a template molecule and CV as the selected electrochemical technique. This synthesis proceeds in four sequential stages as shown in Scheme 1 and described below:

(1) Cysteamine layer self-assembly at the gold working electrode's surface;
(2) CA-125 incubation at the gold working electrode's surface to promote the protein adsorption;
(3) PPy thin film formation leading to CA-125 imprinting at the electrode's surface;
(4) Imprinted CA-125 and excess monomer removal by the use of SDS solution.

To prepare stage 1, the Au-SPE was cleaned through washing with ultra-pure water, acetone and ethanol, before modification by cyclic voltammetry (CV), between 0 and 1.25 V, with a 0.10 V/s scan rate, in a 0.5 mol/L sulfuric acid solution. When the resulting voltamograms from the cycling procedures are the same, it means that the electrode surface is clean (~12 cycles). The electrodes were rinsed with ultra-pure water and dried under a $N_2$ stream.

Stage 1 consists in modification of the woking area of the Au-SPE by self-assembling a cysteamine layer. For that a $25 \times 10^{-3}$ mol/L solution of cysteamine was incubated at the gold electrode for 2 h, at 25 °C. It is well documented the formation of strong interaction between the −SH groups and gold [41], which allows the formation of a compact and stable gold-cysteamine monolayer, with the amine groups ready to bind covalently with the biomarker.

At stage 2, a CA-125 solution (1, 5 and 10 kU/mL were tested) in Phosphate buffer (PB) was incubated at the modified gold electrode for 15 min at 4 °C [22]. The electrodes were then thoroughly rinsed with ultra-pure water. After optimization of this process the concentration of 5 kU/mL was used to prepare the sensors for analytical studies.

Stage 3 consisted in the electropolymerization of Py in the presence of the adsorbed CA-125. This procedure was based on the work of Lu et al. [25] in PB (pH 7.2) containing $1.0 \times 10^{-2}$ mol/L of Py. The electropolymerization was performed by CV at a scan rate of 0.10 V/s between −0.20 V and 1.00 V for defined number of cycles (1, 5, 10 and 15 cycles were tested). After optimization of this process 10 electropolymerization cycles were used to prepare the sensors for analytical studies.

The obtained film was washed with ultra-pure water and stage 4 was performed by incubating the electrode overnight in a $25 \times 10^{-3}$ mol/L sodium dodecyl sulfate solution (SDS). The SDS solution was prepared by dissolving the adequate amount of sodium dodecyl sulfate in a mixture of PB and methanol (10:1, v/v) [40]. Finally, the electrode was abundantly washed with ultra-pure water and dried under a $N_2$ stream to completely remove protein residues from the polymeric film.

As a control, a non-imprinted polymer (NIP) modified Au-SPE was also prepared following the same procedure adopted for the MIP construction, however NIP was prepared in the absence of CA-125 during the electropolymerization process.

### 2.2. Assembly of the MIP-SPR sensor

Assembly and test of the MIP-SPR sensor was performed after optimization of the experimental parameters of MIP construction at the gold SPE electrodes.

The gold SPR sensor surface was washed with ethanol and rinsed with ultra-pure water and dried at room temperature. The clean Au sensor was assembled in the SPR-electrochemical cell with two independent cuvettes. Prior to the electropolymerization, 120 μL of $25 \times 10^{-3}$ mol/L solution of cysteamine was added to the electrochemical cuvette for 2 h at 20 °C. The *in situ* measurements were performed using an Autolab coupled with a SPR instrument, allowing the formation of the imprinted polymer films onto an electrode optical transducer surface (SPR Au substrate). The gold surface plasmon resonator was used as working electrode in a standard three-electrode cell setup with an Ag/AgCl wire as the reference electrode and platinum as the counter electrode. The CA-125 imprinted Py MIP surface was performed using cyclic voltammetry in the potential range between −0.20 V and +1.00 V (*vs.* Ag/AgCl) at a scan rate of 0.050 V/s with a solution containing 5 kU/mL of CA-125 and $1.0 \times 10^{-2}$ mol/L of Py. The CA-125 imprinted and the non-imprinted surface obtained were washed with PB and then incubated overnight with a solution of SDS $25 \times 10^{-3}$ mol/L.

Please refer to Supplementary Material for Apparatus, Reagents and solutions, Electrochemical measurements, Optical measurements and Determination of CA-125 in artificial serum.

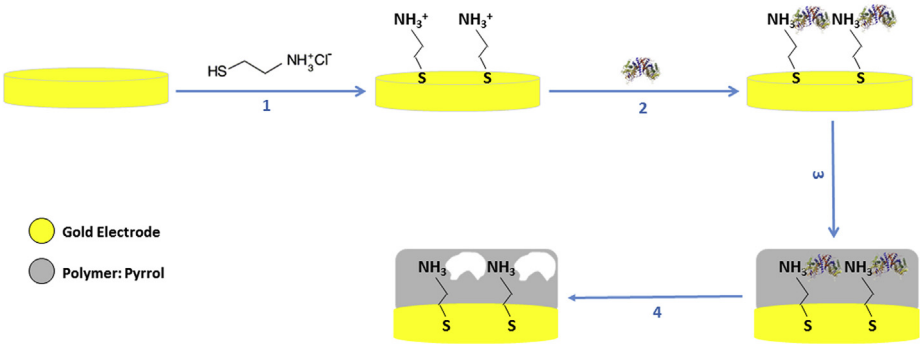


**Scheme 1.** Graphical representation of the different stages of MIP assembly.

## 3. Results and discussion

### 3.1. Optimization of MIP construction

The optimization of the MIP construction focused in three experimental parameters namely, CA-125 template concentration (stage 2), number of CV cycles for electropolymerization (stage 3) and template removal (stage 4). In order to follow the changes produced in the different optimization processes Electrochemical Impedance Spectroscopy (EIS) was selected and $[Fe(CN)_6]^{4-}$/$[Fe(CN)_6]^{3-}$ equimolar solution was used as redox probe.

EIS is used in this optimization process since it is very sensitive to the chemical and physical changes that induce modification in the electron transfer at the interface between electrode and solution. In the present case since the electrochemical transfer is strongly impeded, giving rise to large charge transfer resistance (Rct). The semicircle observed at Nyquist plots indicated a charge-transfer controlled process, where the diameter is equaled the Rct [42]. To extract Rct values the tools available at FRA module of GPES 4.9 software were used.

EIS measurements were performed after polymerization and MIP after formation for different template concentrations, scanning at 0.10 V/s between −0.20 V and 1.00 V and 10 cycles, followed by extraction of template with $25 \times 10^{-3}$ mol/L SDS, are shown in Fig. 1. For comparison, NIP surfaces prepared in absence of template was also included as Fig. 1**D**.

After electropolymerization with Py using 1 kU/mL of template CA-125 resulted in the formation of a high insulating medium at the Au-SPE surface, resulting in high Rct (Fig. 1 A - curve 1) while, after the extraction of the imprinted template (MIP), a large decrease of Rct was observed (Fig. 1 A - curve 2). The Rct numerical values can be found in Table S1 of the supplementary material file.

Results show a consistent increase in the charge transfer resistance after polymerization in the presence of the CA-125 template and a reduction of Rct after the extraction of the imprinted template. Rct values increase when the CA-125 concentration increases from 1 kU/mL (Fig. 1 A) to 5 kU/mL (Fig. 1 B) however, going from 5 to 10 kU/mL (Fig. 1C) the Rct value is practically unchanged. Taking into account the results displayed in Fig. 1, it was decided to use 5 kU/mL of CA-125 as the chosen template concentration, mainly because this offer a more economical way to prepare the CA-125 MIP sensors without compromising the performance.

Results obtained for the NIP presents a similar behavior, with significantly lower Rct values (Fig. 1D).

In order to evaluate the impact of the number of cycles in the electropolymerization process on the MIP performance, EIS measurements were carried out at fixed concentration of immobilized template, 5 kU/mL, and extraction of template with $25 \times 10^{-3}$ mol/L SDS. The experimental results are shown in Fig. 2. The Rct numerical values can be found in Table S2 of the supplementary material file.

The $R_{ct}$ value extracted from the curve represented in Figure **C** (curve **1**) is higher than those in **A** and **B**, which may indicate a more efficient electropolymerization process, leading to a more compact polymer film. Although the surface is thicker, it was possible to remove the protein to obtain the MIPs. A trial was made with 15 cycles, however a blocking surface was obtained no useful MIP could be obtained (results not shown).

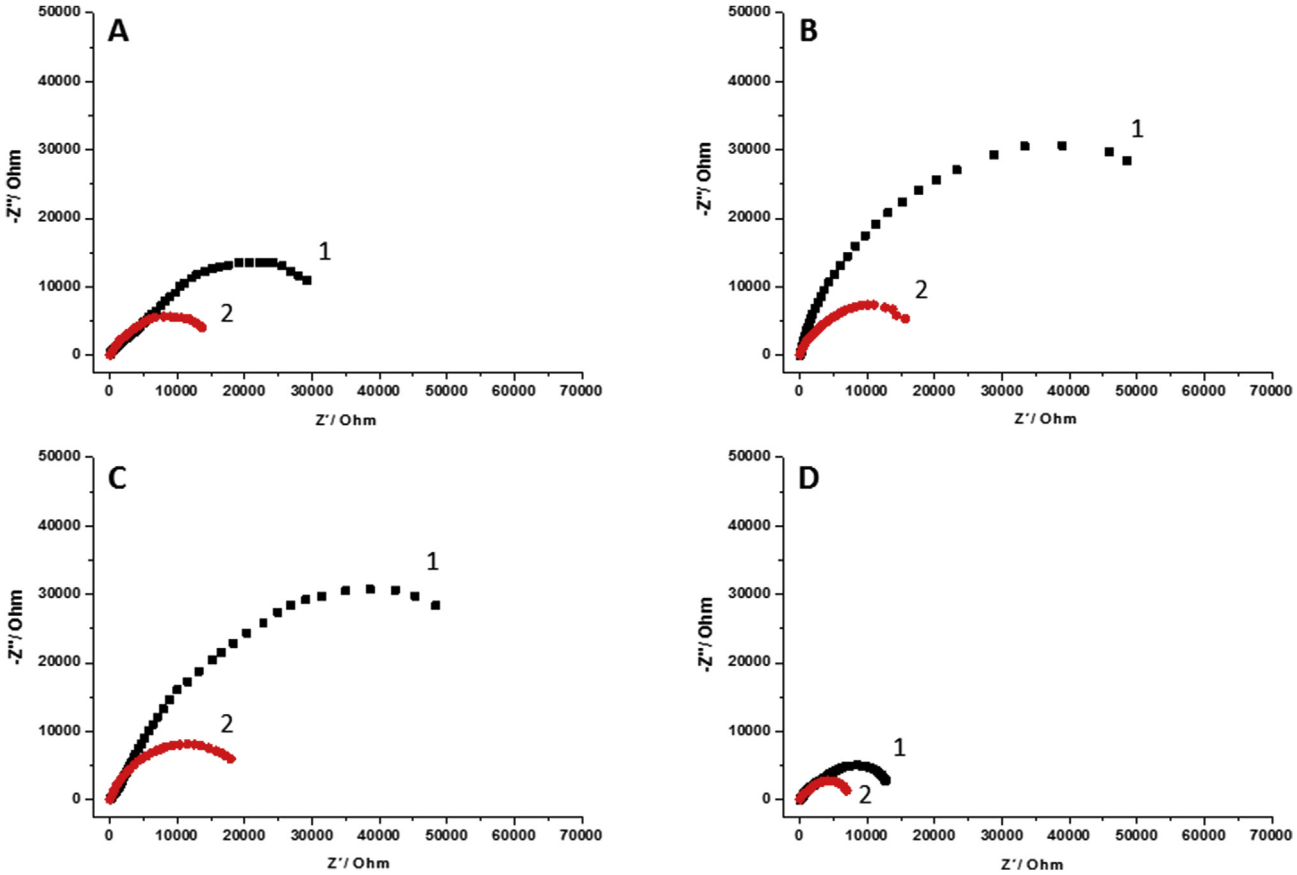


**Fig. 1.** EIS study obtained in 5.0 mM $[Fe(CN)_6]^{3-}$ and 5.0 mM $[Fe(CN)_6]^{4-}$, at 0,12 V, in PB, after polymerization (curve **1**) and after formation of MIP (curve **2**) for different template concentrations: **A**- 1 kU/mL, **B**- 5 kU/mL and **C**- 10 kU/mL. **D**- For comparison, data obtained at NIP surface in the absence of CA-125 was also included in the figure.

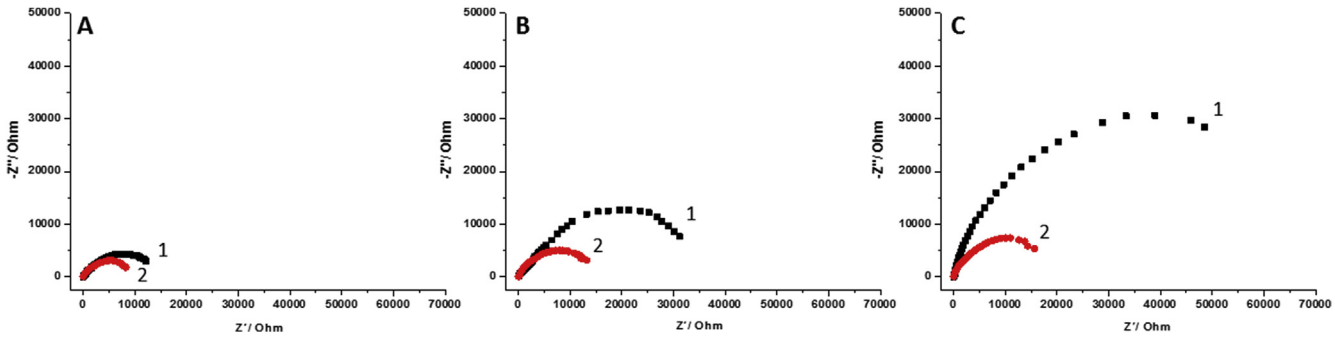


**Fig. 2.** EIS study obtained in 5.0 mM $[Fe(CN)_6]^{3-}$ and 5.0 mM $[Fe(CN)_6]^{4-}$, at 0,12 V, in PB, after polymerization (curve **1**) and after formation of MIP (curve **2**) for different number cycles: **A**- 1 cycle, **B**- 5 cycles and **C**- 10 cycles.

Two strategies were followed in this work to evaluate the effective extraction of CA-125 (stage 4) from the imprinted surface, using $H_2SO_4$ [43] and SDS solutions [40]. The results were compared and are represented in Fig. 3. The Rct numerical values can be found in Table S3 of the supplementary material file.

The results obtained show that SDS solution is the most effective for removal of the template. However, comparing NIP—**B** (curve-2) with MIP-**B** (curve-1), it is possible to observe an increase in the $R_{ct}$ value, which may indicate a possible change in the surface characteristics of the Au-SPE electrode introduced by the $H_2SO_4$.

Thus, the experimental conditions that include the use of 5 kU/mL template concentration, electropolymerization with 10 cycles and an extraction of template with a SDS solution, were considered the optimal conditions to enhance the performance of the biosensor.

### 3.2. Optimization of MIP-SPR construction

Surface plasmon resonance has been used to monitor variations of the refractive index in the vicinity of metal surfaces. The angle at which occurs the maximum loss of the reflected light is called resonance angle or SPR angle. Accordingly, in this study, we used the SPR technique to monitor and characterize the surface imprinting process of CA-125 onto the Au-SPR based sensor. In this work, the main aim of using SPR technique is to obtain complementary data to those obtained and reported in the electrochemical characterization in all steps involving the MIP formation.

The molecularly imprinted polymer-modified Au-SPR surface was developed in three stages including (1) modification of Au surface with cysteamine; (2) electropolymerization of PPy in the presence of the CA-125 template molecule; and (3) removal of CA-125 protein from MIP sensor surface using SDS solution. The several steps were followed using SPR reflectivity measurements and are represented in Fig. 4.

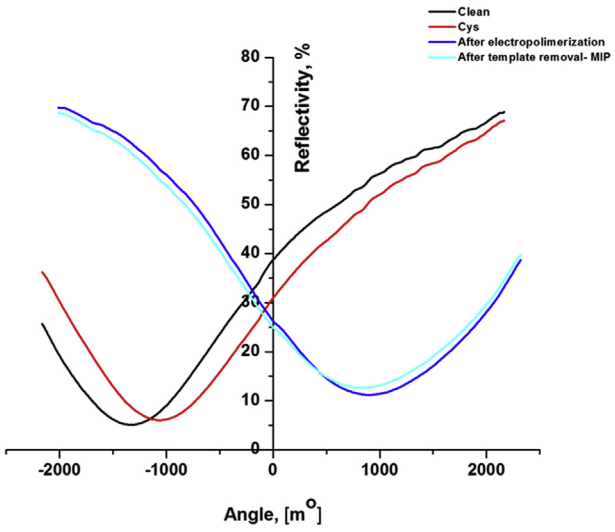


**Fig. 4.** Typical SPR dip curves of the modification steps in the surface of Au-SPR sensor, in PB.

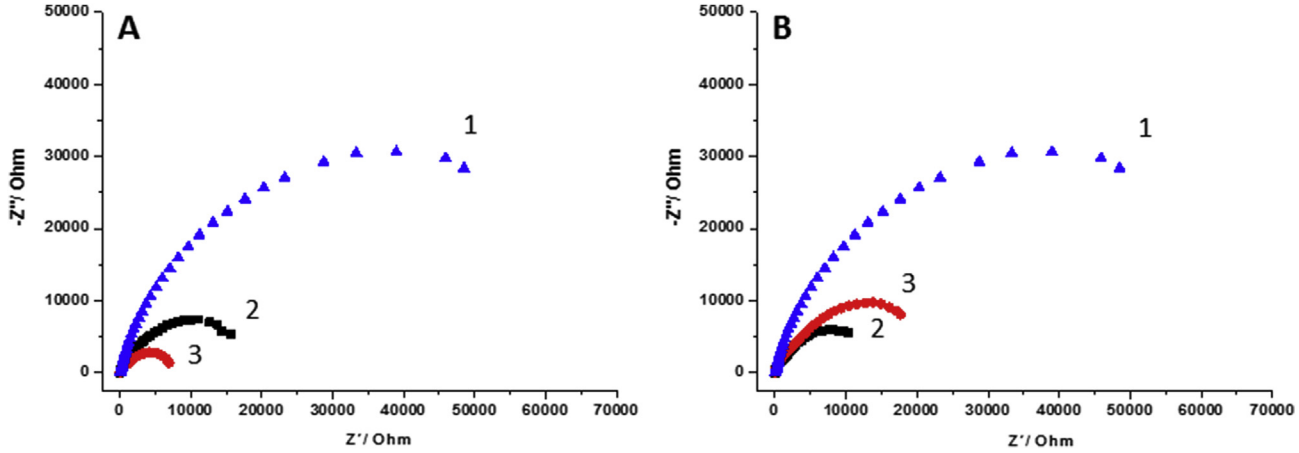


**Fig. 3.** EIS study obtained in 5.0 mM $[Fe(CN)_6]^{3-}$ and 5.0 mM $[Fe(CN)_6]^{4-}$, at 0,12 V, in PB buffer, after polymerization (curve **1**), MIP (curve **2**) and NIP (curve **3**) for different extraction of template: **A**- SDS and **B**— $H_2SO_4$.

The properties of the polymer film used to construct the molecularly imprinted templates are crucial for the sensing performance. In this work, the SPR technique was applied in order to monitor the changes of the refractive index at a solid–liquid interface in all stages of the MIP construction. Typical SPR curves obtained in the MIP at 20 °C are represented in Fig. 4. The first step, that precedes the molecularly imprinted CA-125 grafted in PPy film step, consists in the modification of the SPR Au surface with cysteamine. Cysteamine has been extensively used in the immobilization of proteins or peptides onto SPR gold surfaces in order to have a controlled orientation through the establishment of covalent Au–S bonds [44]. The Au - thiol group (–SH) bond induced a shift of 234 m° in the SPR angle compared with the bare Au SPR dip angle measured with PB supporting electrolyte.

Comparing the SPR angles obtained in the clean sensor or after modification of cysteamine with SPR dip profiles measured after the electropolymerization, it is clear that modification with MIP occurred since an effective shift of the SPR dip to more positives angles was observed, reflecting the change in refractive index near the SPR Au surface (dip cysteamine: 1114 m°, and dip MIP: + 875 m°).

The subsequent step to the MIP construction process is the removal of the CA-125, which was carried out to create the imprinted binding sites. The performance of the SPR sensor platform prepared is crucially dependent on the effective removal of the template target molecule, in order to maintain the integrity of the cavities namely the chemical template functionality [45]. For this purpose, a solution of SDS was added to the imprinted polymer film in order to release the template molecule from the polymer film. The surface plasmon angle position shift ($\Delta\theta$) obtained after the template removal was approximately 57 m° and a slight increase in the reflectivity has occurred, producing a slight decrease in the refractive index at the sensor surface.

The Au-SPR sensor based on molecularly imprinted PPy was prepared *in situ* in the SPR cuvette coupled to a potentiostat for the determination of CA-125 biomarker using a SPR transduction. The molecularly imprinted surface was prepared by incorporation of the CA-125 during the electropolymerization of Py on Au-SPR sensor in PB buffer solution using CV method. As a control, a NIP was also prepared. The NIP film was prepared according to the procedure described for the MIP construction however, in the absence of the template molecule. These results can be found in the supplementary material file Fig. S1.

### 3.3. Surface characterization by AFM the surface of Au-SPE

The surface characterization was made directly over the surface of Au-SPEs. The AFM images were obtained in the clean Au-SPE, after the electropolymerization process and posterior extraction of CA-125 template from the polymer. The images are represented in Fig. 5.

The clean Au-SPE electrode has the root mean square (RMS) surface roughness of 0.308 μm (**A**), this surface roughness is typical of the gold ink films used in the fabrication of Au-SPEs electrodes. After the electropolymerization process, the value of RMS decreases to 0.252 μm (**B**) which can be interpreted as the formation of a polymeric network on the electrode surface that contributes to the surface smoothing. Finally, after extraction of template CA-125 of polymer with SDS, the RMS value increases to 0.278 μm (**C**), which can be interpreted as an increase in the film roughness induced by the CA-125 removal from the polymer network.

### 3.4. Analytical response of CA-125 biosensor electrochemical

SWV technique was used for CA-125 quantification, presenting high sensitivity to the surface's reaction, suitable detection capabilities and allowing fast data acquisition.

The calibration curve plots the current intensity (I) against logarithm of the CA-125 concentration, ranging from 0.01 to 1000 U/mL (Fig. 6).

The presence of CA-125 in the redox probe increased the current of the anodic peak at ~0.2 V on Au-SPE surface. From the analysis of Fig. 6, a linear pattern against Log [CA-125] was observed for concentrations ranging from 0.01 to 500 U/mL, with a correlation coefficient 0.986.

The limit of detection (LOD) obtained by the MIP sensor was estimated according to the international recommendations for ion-selective electrodes [46]. The LOD obtained in this work (0.01 U/mL), is lower than most of the sensors reported in literature using different analytical methods (see Supplementary Material

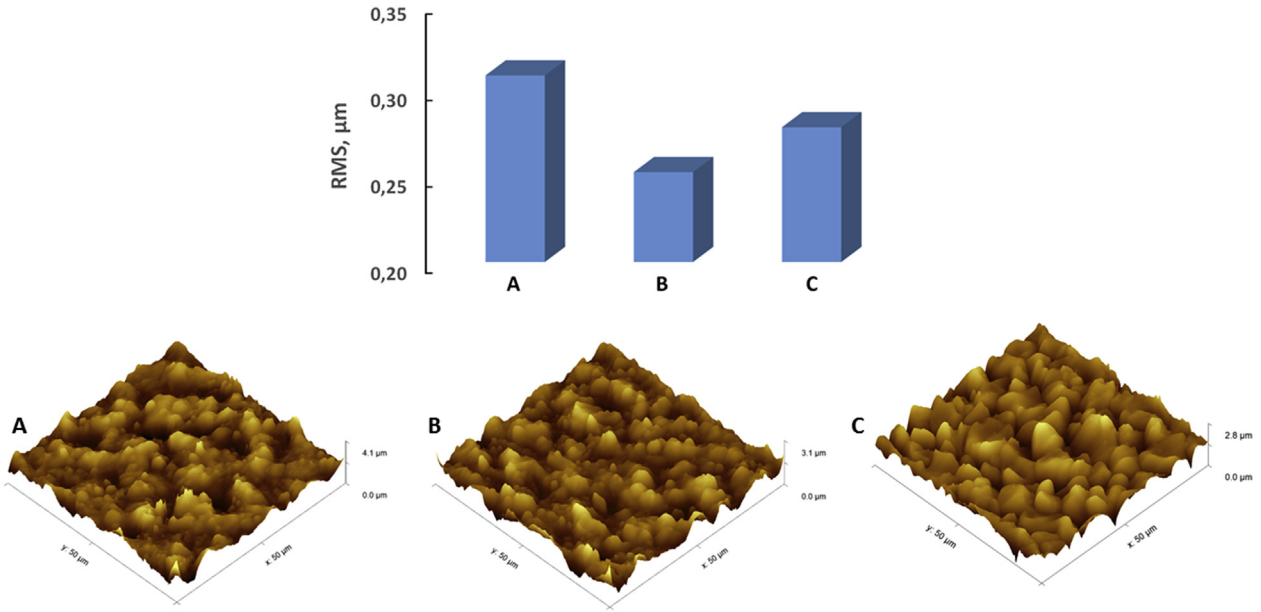


**Fig. 5.** AFM images for the different modification of surface Au-SPE electrode. **A**- Clean Au-SPE, **B**- After electropolymerization and **C**- MIP.

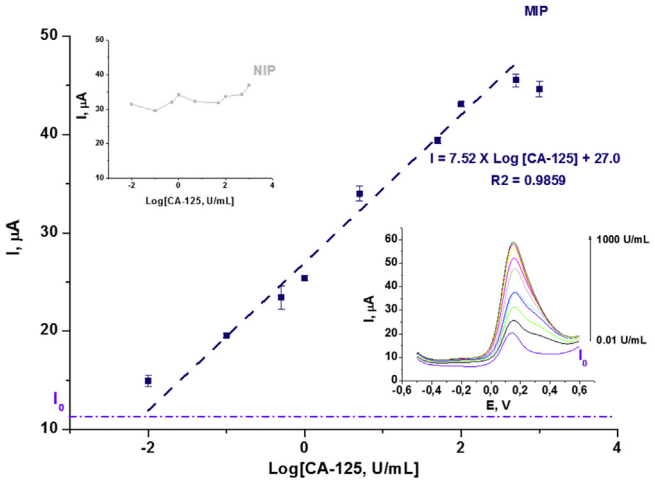


**Fig. 6.** Calibration curves of MIP and NIP based Au-SPE biosensor obtained by SWV measurements in 5.0 mM $[Fe(CN)_6]^{3-}$ and 5.0 mM $[Fe(CN)_6]^{4-}$ in PB. Inset: SWV measurements of MIP based Au-SPE biosensor.

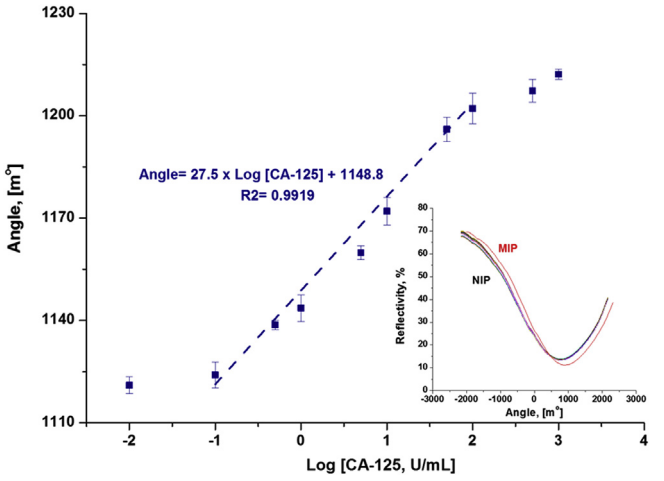


**Fig. 7.** Resonance angle shift of MIP/optical sensor chips according to varying concentrations of the CA-125 solution. In the insert is represented the comparison of SPR dips obtained for the NIP surface (different concentrations of CA-125 and the SPR dip obtained for the CA-125 imprinted surface).

Table S4). There are three exceptions, the first one presented in the Field Effect Transitor (FET) - type aptasensor work that has LOD 0.5 nU/mL [47], where the recognition element is an aptamer, the second and third are immunosensors based, respectively in electrochemiluminescence with LOD of 0.4 mU/mL [48] and in electrochemical and colorimetric sensor with LOD of 5 mU/mL [49]. Albeit the lower value of LOD, the linear range ends at concentrations that are below the lower threshold of CA-125 in healthy donors.

It was possible to find another electrochemical biosensor in the literature, that used a MIP as biorecognition element MIP, with LOD 0.5 U/mL [22]. This value is 50 times higher than the LOD reported in this work and the previous MIP-SPE sensor presents only 4 decades of linear range while the sensor described in the present work displays 6 decades of linear range.

From examination of available data for CA-125 analysis it is evident that the coefficient of determination is usually (with few exceptions) bellow 0.99 (please see Supplementary Material Table S4). This could be associated with the purity of the commercially available biomarker.

Although MIP- based sensors are usually considered as a single use sensor, it was possible to reuse the MIP-based sensors developed in this work, although this is an aspect that has to be improved. The developed biosensor was stored at 4 °C and under these conditions the biosensor can be reused twice, offering a stable response, with an average relative standard deviation of 5% over the first use. For this, the biosensor has to be cleaned with SDS ($25 \times 10^{-3}$ mol/L) overnight and subsequent washing with ultrapure water.

### 3.5. Analytical response of CA-125 optical biosensor

An imprinted SPR sensor selective for CA-125 was successfully obtained. MIP-based optical sensors may enable higher sensitivity, label-free detection, real-time monitoring, low volume sample consumption and in addition, can become a cost-effective solution to antibody-antigen recognition/detection methods.

The response to CA-125 was assessed using an optical transducer via surface plasmon resonance. CA-125 was diluted in PB and injected in a range of concentrations from 0.01 to 1000 U/mL in order to determine the sensitivity of the method. The performance of the imprinted and non-imprinted surface was evaluated by monitoring the change in the SPR angle as a function of the log |CA-125| and the trend is represented in Fig. 7. Regarding the analyte's detection, SPR has been considered as an efficient technique which has the advantage in providing a real-time monitoring over other analytical procedures.

Once CA-125 was added into the channel system, it bounds to the MIP template on the surface of the modified gold disk and the SPR signal increased within a linear interval while higher concentrations gave a constant response due to the probable saturation of the sensor Fig. 7.

These results suggest that the combination of SPR sensing with a PPy film as a synthetic receptor can be used to detect CA-125. The CA-125 binding to the recognition element resulted in a physical change that was transduced into a change of optical properties e.g. change in refractive index occurring within approximately a few hundred nanometers from the sensor surface. The calibration curve for CA-125 represented in Fig. 7 was built by plotting the SPR angle shift *vs*. logarithm of the concentration, showing linearity at CA-125 concentrations ranging from 0.1 to 300 U/mL ($R^2 = 0.992$) with a LOD > 0.1 U/mL. These results suggest that molecular imprinting can be applied to the detection of CA-125 using the SPR as a transducer, e.g., the combination of SPR sensing with molecular imprinting technology is a potential method for the detection of carbohydrate antigen 125.

In the inset of Fig. 7, it is clear that the angular shift value is higher during the CA-125 PPy film preparation (angular shift ~+875 m°) than the NIP (~+737 m°), indicating that more material is being deposited during MIP film formation. Results also showed higher binding affinity of CA-125 for the MIP sensor than for the NIP sensor indicating good specificity.

This method showed a similar detection limit (0.1 U/mL) to that obtained by using a SPR immunosensor with anti-CA-125 immobilized on gold surface through a self-assembled monolayer [50]. The immunosensor developed by Suwansa-ard et al. [50] was based on flow injection label-free detection for CA-125 in human serum samples. The limit of detection obtained by this technique was slightly higher compared to a capacitive immunosensor using the same immobilization technique however, the SPR method allows a more accurate real-time monitoring of the immobilization and optimization steps.

### 3.6. Studies of binding isotherm

Binding affinity in the MIP system for the electrochemical and optical biosensor were evaluated by adjusting the experimental data to the Freundlich isotherm using equation (1) [51]:

$$q_e = K_F \times C_e^{\frac{1}{n_F}} \quad (1)$$

Where $q_e$ is the adsorbed amount at equilibrium and is calculated as $(I_0-I)/I_0$ or $(\theta_0-\theta)/\theta_0$ in the case of electrochemical or optical data respectively. $C_e$ (U/mL) is the equilibrium concentration, $K_F$ and $n_F$ are the Freundlich constants related to adsorption capacity and adsorption intensity, respectively. If $n_F > 1$, suggesting favorable adsorption, then adsorption capacity increases [52].

A Langmuir- Freundlich isotherm was also tested, however the chi-squared values were similar for both isotherms and therefore only the Freundlich isotherm data is presented. The binding isotherms for MIP/electrochemical and MIP/optical are presented in Fig. 8.

From equation (1) it was estimated for the MIP/electrochemical a $n_F$ value of $6.54 \pm 0.76$ and a $n_F$ of $29.6 \pm 4.3$ for the MIP/optical sensor. Both values of $n_F$ assessed were found to be > 1 suggesting a favorable adsorption. The MIP/electrochemical presents a better adsorption capacity, because it presents higher $K_F$ value ($1.30 \pm 0.11$ U/mL) as compared to MIP/optical ($0.29 \pm 0.01$ U/mL). The results obtained are in line with the expected behavior for MIP and NIP isotherms [53]. Ribeiro et al. [40] also presented a comparison between MIP and NIP binding behavior showing a higher $K_F$ value for MIP which is an indications better bounding. A tenfold increase in the adsorption capacity of CA-125 to MIP/electrochemical as compared to the MIP/optical, demonstrated the effectiveness of this approach in creating a high affinity synthetic receptor for the target biomarker. Differences in the isotherm parameters between MIP/electrochemical and MIP/optical can also be understood if we take in to account the differences in surface roughness of the gold layer between the SPR gold disk and the gold film in SPE. Furthermore, the MIP/optical is only sensitive to the CA-125 molecules that can pass through the polymer network but are adsorbed at the gold electrode while, in the MIP/electrochemical, due to the use of an electrochemical probe, even those CA-125 molecules that are further away from the surface can be detected using this methodology.

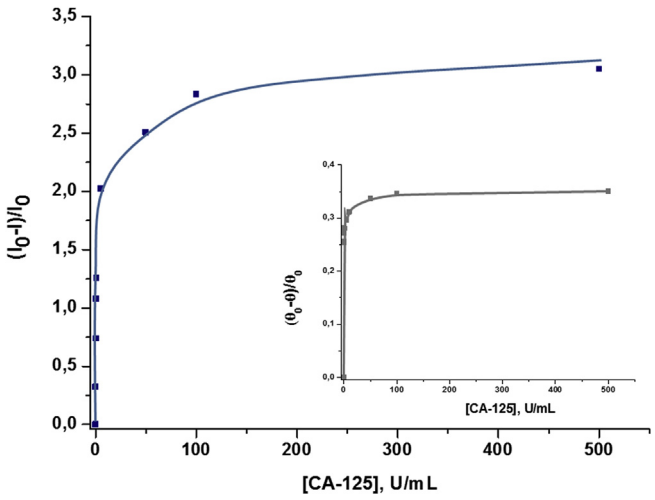


**Fig. 8.** Binding isotherm of synthetic MIP/electrochemical receptor film at different concentrations of CA-125. Inset: Binding isotherm of synthetic MIP/optical receptor film. The lines represent the fitting of Freundlich isotherm to the experimental data.

Comparing the previous reported analytical parameters such as the binding isotherm for MIP performance and analytical calibration for both transduction methods, the electrochemical biosensor setup presented better performance and therefore it was selected to proceed the study of selectivity and quantification of CA-125 biomarker in artificial serum.

### 3.7. Interference studies

The study of sensor selectivity has great importance in the application of this sensor for the quantification of the target biomarker. The sensor surface is exposed to different species that may be present in biological fluids. The species that can be found in the serum may interfere with the quantification of the biomarker in biological samples. The ethical issues that may arise in studies involving biological samples and also regulatory aspects regarding authorizations make it difficult to obtain and apply real samples in the laboratory context. Consequently, the analytical performance study of the sensor was performed in artificial serum medium, in order to compare analytical performance features of sensor with those obtained in buffer (PB). The artificial serum considered in the present study was prepared with a similar composition of the serum from biological samples [54]. Artificial serum was diluted 10 times before preparation of the CA-125 standard solutions. (See supplementary material file for details on the preparation of the artificial serum).

The level of interference from the artificial serum components can be evaluated comparing the linear ranges, slopes and the LODs obtained through the calibration curves of MIP in PB and MIP sensor in contact with artificial serum. The results obtained are presented in Table 1.

The results obtained showed that the MIP sensor in contact with artificial serum increased sensitivity (11.06 μA/decade), LOD (0.1 U/mL) and the linear concentration range narrowed from 0.1 to 500 U/mL. Even with the narrowing of the working range, the quantification of CA-125 in the serum is possible, since its threshold value is 35 U/mL.

As a complement to this study, the quantification of breast cancer biomarker Carbohydrate Antigen 15–3 (CA-15-3) [55,56] was performed with the MIP-based biosensor developed in this work in PB, to evaluate the effect of the presence of an analog carbohydrate antigen as a probable interferent in the CA-125 molecular recognition. The calibration curve obtained is presented in Fig. 9 for the concentration range of CA-15-3 between 0.01 and 1000 U/mL. A linear trend was obtained from the plot for concentrations ranging from 1 to 500 U/mL, with a correlation coefficient 0.984 and a sensitivity of 0.798 μA/decade, as showed in the inset of Fig. 9. From the data analysis, it is possible to conclude that the proposed MIP-based electrochemical biosensor showed good selectivity against interfering compounds such as the biomarker CA-15-3 and major components of serum.

The quantification of CA-125 samples was made with the MIP-based electrochemical biosensor in the artificial serum media, considering blank samples of artificial serum being spiked with CA-125 in order to obtain concentrations between 0.2 and 150 U/mL.

**Table 1**
Calibration features of the biosensor in the PB and artificial serum.

| Characteristics | MIP | |
|---|---|---|
| | PB | Serum |
| Slope (μA/decade) | 7.52 | 11.06 |
| LOD (U/mL) | 0.01 | 0.1 |
| $R^2$ | 0.986 | 0.992 |
| Linear concentration range (U/mL) | 0.01–500 | 0.1–500 |

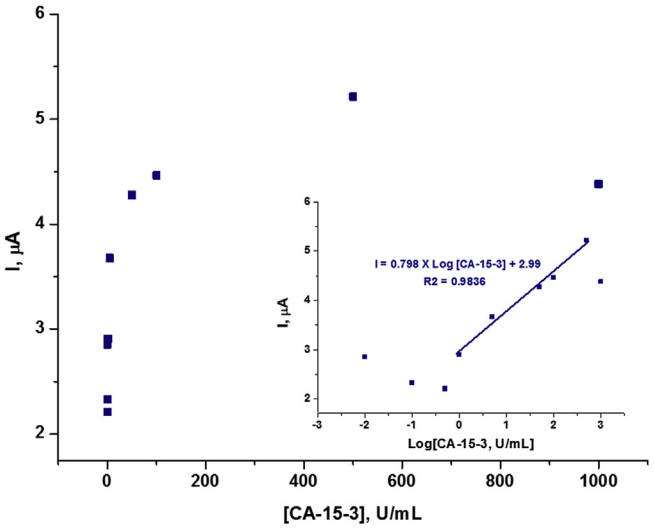


**Fig. 9.** Calibration curve obtained of MIP the CA-125 biosensor obtained by SWV measurements in 5.0 mM $[Fe(CN)_6]^{3-}$ and 5.0 mM $[Fe(CN)_6]^{4-}$ in PB for quantification of biomarker CA-15-3. Inset: Linear calibration plot obtained for CA-15-3.

**Table 2**
Determination of CA-125 in artificial serum.

| Sample | CA-125 (U/mL) | Found (U/mL) | Recovery (%) | Relative error (%) |
|---|---|---|---|---|
| 1 | 0.2 | 0.21 ± 0.01 | 105 ± 6 | 5.0 |
| 2 | 3 | 2.8 ± 0.3 | 93 ± 6 | −6.7 |
| 3 | 30 | 27 ± 3 | 91 ± 5 | −9.3 |
| 4 | 150 | 153.5 ± 0.3 | 102 ± 6 | 2.3 |

The results obtained for four samples in triplicate with different concentration levels are summarized in Table 2.

The results show that there is a good relationship between added and found amounts of CA-125. The overall recoveries measured ranges from 91 to 105% with an average relative error of 5.8%. The experimental results revealed that the proposed imprinted biosensor can be successfully applied for the detection of CA-125 target molecule in diluted human serum samples providing reliable results in real samples.

## 4. Conclusions

This work presents the development and optimization of an efficient electrochemical biosensor, for the determination of CA-125 biomarker in artificial serum based on the molecular imprinting technology, through simple electropolymerization of Py. A comparison between electrochemical and optical (SPR) sensors platforms revealed that the performance of the SPR sensor is similar to that previously described in the literature and that the electrochemical sensor presented a better performance (lower LOD and larger linear range).

The biosensor developed in this study presented good analytical performance, improving previously published MIP based electrochemical sensor, such as larger concentration linear range (0.01 and 500 U/mL), low LOD (0.01 U/mL), good selectivity and sensitivity. The biosensor was successfully applied to the analysis of CA-125 in artificial serum samples, showing good sensitivity and selectivity and presenting similar or better performance than colorimetric and fluorometric sensors found in the literature.

The CA-125 biomarker has a threshold value of 35 U/mL expressed by more than 80% of patients with non-mucinous epithelial ovarian cancer and the biosensor associated to the molecularly imprinted technology seems to bring a simple strategy for a low detection limit analysis of biomolecules with high molecular weight (200–1000 kD).

Although efforts have to be done in order to increase the robustness of the polymer film, allowing to reuse the MIP-SPE sensor, the proposed biosensor has the potential to become an excellent candidate for monitoring CA-125 and to be further used in practical clinic cancer diagnosis, as a valuable resource for CA-125 detection in point-of-care.

## Conflict of interests

The authors declare that they have no known conflict of interests.

## Declaration of competing interest

The authors declare that they have no known competing financial interests or personal relationships that could have appeared to influence the work reported in this paper.

## Acknowledgements

This research had the financial support of FCT (Fundação para a Ciência e Tecnologia), Portugal, and co-financed by the FEDER funds, European Union, under the Partnership Agreement PT2020, through project POCI/01/0145/FEDER/006980 with reference UID/QUI/UI0081/2019 (CIQUP), by NORTE-2020 and COMPETE 2020, Portugal, through projects NORTE-01-0247-FEDER-017834 (RAMSERS) and NORTE-01-0145-FEDER-000028 (SAM).

## Appendix A. Supplementary data

Supplementary data to this article can be found online at https://doi.org/10.1016/j.aca.2019.07.050.

## References

[1] Globocan Cancer, Estimated Cancer Incidence, Mortality and Prevalence Worldwide in 2012, 2012.
[2] R. Siegel, D. Naishadham, A. Jemal, Cancer statistics, 2013, CA A Canc. J. Clin. 63 (2013) 11–30.
[3] R.C. Bast, M. Feeney, H. Lazarus, L.M. Nadler, R.B. Colvin, R.C. Knapp, Reactivity of a monoclonal antibody with human ovarian carcinoma, J. Clin. Investig. 68 (1981) 1331–1337.
[4] F. Leung, M.Q. Bernardini, M.D. Brown, Y. Zheng, R. Molina, R.C. Bast, G. Davis, S. Serra, E.P. Diamandis, V. Kulasingam, Validation of a novel biomarker panel for the detection of ovarian cancer, Cancer Epidemiol. Biomark. Prev. 25 (2016) 1333.
[5] M. Johari-Ahar, M.R. Rashidi, J. Barar, M. Aghaie, D. Mohammadnejad, A. Ramazani, P. Karami, G. Coukos, Y. Omidi, An ultra-sensitive impedimetric immunosensor for detection of the serum oncomarker CA-125 in ovarian cancer patients, Nanoscale 7 (2015) 3768–3779.
[6] A. Ravalli, G.P. dos Santos, M. Ferroni, G. Faglia, H. Yamanaka, G. Marrazza, New label free CA125 detection based on gold nanostructured screen-printed electrode, Sens. Actuators B Chem. 179 (2013) 194–200.
[7] S. Viswanathan, C. Rani, C. Delerue-Matos, Ultrasensitive detection of ovarian cancer marker using immunoliposomes and gold nanoelectrodes, Anal. Chim. Acta 726 (2012) 79–84.
[8] J. Das, S.O. Kelley, Protein detection using arrayed microsensor chips: tuning sensor footprint to achieve ultrasensitive readout of CA-125 in serum and whole blood, Anal. Chem. 83 (2011) 1167–1172.
[9] D. Tang, L. Hou, R. Niessner, M. Xu, Z. Gao, D. Knopp, Multiplexed electrochemical immunoassay of biomarkers using metal sulfide quantum dot nanolabels and trifunctionalized magnetic beads, Biosens. Bioelectron. 46 (2013) 37–43.
[10] S. Ge, L. Ge, M. Yan, X. Song, J. Yu, S. Liu, A disposable immunosensor device for point-of-care test of tumor marker based on copper-mediated amplification, Biosens. Bioelectron. 43 (2013) 425–431.
[11] A. Raamanathan, G.W. Simmons, N. Christodoulides, P.N. Floriano, W.B. Furmaga, S.W. Redding, K.H. Lu, R.C. Bast, J.T. McDevitt, Programmable bio-nano-chip systems for serum CA125 quantification: towards ovarian cancer diagnostics at the point-of-care 5, Cancer prevention research,

Philadelphia, Pa, 2012, pp. 706–716.
[12] S.-H. Sun, M.-J. Lee, Y.-H. Lee, W. Lee, X. Song, C.-Y. Chen, Immunoassays for the cancer biomarker CA125 based on a large-birefringence nematic liquid-crystal mixture, Biomed. Opt. Express 6 (2015) 245–256.
[13] J.V. Jokerst, A. Raamanathan, N. Christodoulides, P.N. Floriano, A.A. Pollard, G.W. Simmons, J. Wong, C. Gage, W.B. Furmaga, S.W. Redding, J.T. McDevitt, Nano-bio-chips for high performance multiplexed protein detection: determinations of cancer biomarkers in serum and saliva using quantum dot bioconjugate labels, Biosens. Bioelectron. 24 (2009) 3622–3629.
[14] R.C. Bast, T.L. Klug, E.S. John, E. Jenison, J.M. Niloff, H. Lazarus, R.S. Berkowitz, T. Leavitt, C.T. Griffiths, L. Parker, V.R. Zurawski, R.C. Knapp, A radioimmunoassay using a monoclonal antibody to monitor the course of epithelial ovarian cancer, N. Engl. J. Med. 309 (1983) 883–887.
[15] B.W.T. Yin, K.O. Lloyd, Molecular cloning of the CA125 ovarian cancer antigen: Identification as a new MUCIN, MUC16, J. Biol. Chem. 276 (2001) 27371–27375.
[16] K. Sjövall, B. Nilsson, N. Einhorn, The significance of serum CA 125 elevation in malignant and nonmalignant diseases, Gynecol. Oncol. 85 (2002) 175–178.
[17] A.P.F. Turner, Biosensors: sense and sensibility, Chem. Soc. Rev. 42 (2013) 3184–3196.
[18] G. Vasapollo, R. Del Sole, L. Mergola, M.R. Lazzoi, A. Scardino, S. Scorrano, G. Mele, Molecularly imprinted polymers: present and future prospective, Int. J. Mol. Sci. 12 (2011) 15908–15945.
[19] T.S.C.R. Rebelo, C. Santos, J. Costa-Rodrigues, M.H. Fernandes, J.P. Noronha, M.G.F. Sales, Novel Prostate Specific Antigen plastic antibody designed with charged binding sites for an improved protein binding and its application in a biosensor of potentiometric transduction, Electrochim. Acta 132 (2014) 142–150.
[20] F.T.C. Moreira, S. Sharma, R.A.F. Dutra, J.P.C. Noronha, A.E.G. Cass, M.G.F. Sales, Protein-responsive polymers for point-of-care detection of cardiac biomarker, Sens. Actuators B Chem. 196 (2014) 123–132.
[21] X. Qin, H. Xiao-Ya, H. Shi-Rong, Electrochemical Sensors Based on Electropolymerized Films, in: E. Schab-Balcerzak (Ed.) Electropolymerization2011, pp. 226.
[22] S. Viswanathan, C. Rani, S. Ribeiro, C. Delerue-Matos, Molecular imprinted nanoelectrodes for ultra sensitive detection of ovarian cancer marker, Biosens. Bioelectron. 33 (2012) 179–183.
[23] X. Kan, Z. Xing, A. Zhu, Z. Zhao, G. Xu, C. Li, H. Zhou, Molecularly imprinted polymers based electrochemical sensor for bovine hemoglobin recognition, Sens. Actuators B Chem. 168 (2012) 395–401.
[24] A. Ramanavičius, A. Ramanavičienė, A. Malinauskas, Electrochemical sensors based on conducting polymer—polypyrrole, Electrochim. Acta 51 (2006) 6025–6037.
[25] B. Lu, J. Xia, Z. Wang, F. Zhang, M. Yang, Y. Li, Y. Xia, Molecularly imprinted electrochemical sensor based on an electrode modified with an imprinted pyrrole film immobilized on a [small beta]-cyclodextrin/gold nanoparticles/graphene layer, RSC Adv. 5 (2015) 82930–82935.
[26] X. Xing, S. Liu, J. Yu, W. Lian, J. Huang, Electrochemical sensor based on molecularly imprinted film at polypyrrole-sulfonated graphene/hyaluronic acid-multiwalled carbon nanotubes modified electrode for determination of tryptamine, Biosens. Bioelectron. 31 (2012) 277–283.
[27] L. Özcan, Y. Şahin, Determination of paracetamol based on electropolymerized-molecularly imprinted polypyrrole modified pencil graphite electrode, Sens. Actuators B Chem. 127 (2007) 362–369.
[28] M. Mascini, S. Tombelli, Biosensors for biomarkers in medical diagnostics, Biomarkers 13 (2008) 637–657.
[29] E. Wijaya, C. Lenaerts, S. Maricot, J. Hastanin, S. Habraken, J.-P. Vilcot, R. Boukherroub, S. Szunerits, Surface plasmon resonance-based biosensors: from the development of different SPR structures to novel surface functionalization strategies, Curr. Opin. Solid State Mater. Sci. 15 (2011) 208–224.
[30] P.P. Vachali, B. Li, A. Bartschi, P.S. Bernstein, Surface plasmon resonance (SPR)-based biosensor technology for the quantitative characterization of protein–carotenoid interactions, Arch. Biochem. Biophys. 572 (2015) 66–72.
[31] L. Chen, X. Wang, W. Lu, X. Wu, J. Li, Molecular imprinting: perspectives and applications, Chem. Soc. Rev. 45 (2016) 2137–2211.
[32] E.P.C. Lai, A. Fafara, V.A. VanderNoot, M. Kono, B. Polsky, Surface plasmon resonance sensors using molecularly imprinted polymers for sorbent assay of theophylline, caffeine, and xanthine, Can. J. Chem. 76 (1998) 265–273.
[33] T.R.J. Holford, F. Davis, S.P.J. Higson, Recent trends in antibody based sensors, Biosens. Bioelectron. 34 (2012) 12–24.
[34] J.-F. Masson, Surface plasmon resonance clinical biosensors for medical diagnostics, ACS Sens. 2 (2017) 16–30.
[35] A. Dhanjai, L. Sinha, X. Wu, J. Lu, R. Chen, Jain, Advances in sensing and biosensing of bisphenols: a review, Anal. Chim. Acta 998 (2018) 1–27.
[36] M.L. Yola, T. Eren, N. Atar, Molecular imprinted nanosensor based on surface plasmon resonance: application to the sensitive determination of amoxicillin, Sens. Actuators B Chem. 195 (2014) 28–35.
[37] E. Sari, R. Üzek, M. Duman, A. Denizli, Fabrication of surface plasmon resonance nanosensor for the selective determination of erythromycin via molecular imprinted nanoparticles, Talanta 150 (2016) 607–614.
[38] J. Ashley, Y. Shukor, R. D'Aurelio, L. Trinh, T.L. Rodgers, J. Temblay, M. Pleasants, I.E. Tothill, Synthesis of molecularly imprinted polymer nanoparticles for α-casein detection using surface plasmon resonance as a milk allergen sensor, ACS Sens. 3 (2018) 418–424.
[39] X.-Y. Xu, X.-G. Tian, L.-G. Cai, Z.-L. Xu, H.-T. Lei, H. Wang, Y.-M. Sun, Molecularly imprinted polymer based surface plasmon resonance sensors for detection of Sudan dyes, Anal. Methods 6 (2014) 3751–3757.
[40] J.A. Ribeiro, C.M. Pereira, A.F. Silva, M.G.F. Sales, Electrochemical detection of cardiac biomarker myoglobin using polyphenol as imprinted polymer receptor, Anal. Chim. Acta 981 (2017) 41–52.
[41] F.T.C. Moreira, R.A.F. Dutra, J.P. Noronha, M.G.F. Sales, Novel sensory surface for creatine kinase electrochemical detection, Biosens. Bioelectron. 56 (2014) 217–222.
[42] M.A. Panagopoulou, D.V. Stergiou, I.G. Roussis, M.I. Prodromidis, Impedimetric biosensor for the assessment of the clotting activity of rennet, Anal. Chem. 82 (2010) 8629–8636.
[43] T.S.C.R. Rebelo, C.M. Pereira, M.G.F. Sales, J.P. Noronha, F. Silva, Protein Imprinted Material electrochemical sensor for determination of Annexin A3 in biological samples, Electrochim. Acta 190 (2016) 887–893.
[44] H.H. Nguyen, J. Park, S. Kang, M. Kim, Surface plasmon resonance: a versatile technique for biosensor applications, Sensors 15 (2015).
[45] G. Ertürk, B. Mattiasson, Molecular imprinting techniques used for the preparation of biosensors, Sensors 17 (2017).
[46] R.P. Buck, E. Lindner, Recommendations for nomenclature of ion-selective electrodes (IUPAC Recommendations 1994), Pure Appl. Chem. 66 (1994) 2527–2536.
[47] S. Mansouri Majd, A. Salimi, Ultrasensitive flexible FET-type aptasensor for CA 125 cancer marker detection based on carboxylated multiwalled carbon nanotubes immobilized onto reduced graphene oxide film, Anal. Chim. Acta 1000 (2018) 273–282.
[48] L. Wu, Y. Sha, W. Li, S. Wang, Z. Guo, J. Zhou, X. Su, X. Jiang, One-step preparation of disposable multi-functionalized g-C3N4 based electrochemiluminescence immunosensor for the detection of CA125, Sens. Actuators B Chem. 226 (2016) 62–68.
[49] W. Hong, S. Lee, Y. Cho, Dual-responsive immunosensor that combines colorimetric recognition and electrochemical response for ultrasensitive detection of cancer biomarkers, Biosens. Bioelectron. 86 (2016) 920–926.
[50] S. Suwansa-ard, P. Kanatharana, P. Asawatreratanakul, B. Wongkittisuksa, C. Limsakul, P. Thavarungkul, Comparison of surface plasmon resonance and capacitive immunosensors for cancer antigen 125 detection in human serum samples, Biosens. Bioelectron. 24 (2009) 3436–3441.
[51] H.M.F. Freundlich, Over the adsorption in solution, J. Phys. Chem. 57 (1906) 385–471.
[52] X. He, K.B. Male, P.N. Nesterenko, D. Brabazon, B. Paull, J.H.T. Luong, Adsorption and desorption of methylene blue on porous carbon monoliths and nanocrystalline cellulose, ACS Appl. Mater. Interfaces 5 (2013) 8796–8804.
[53] R.J. Ansell, Characterization of the binding properties of molecularly imprinted polymers, in: B. Mattiasson, L. Ye (Eds.), Molecularly Imprinted Polymers in Biotechnology. Advances in Biochemical Engineering/Biotechnology vol. 150, Springer, Cham, 2015.
[54] K.P.G. Ralloff, P. Westh, R.A. Purssell, M. Pudek, Y. Koga, Non-ideality of methanol solution's of artificial serum in the mole fraction range from 5 x 10(-4) to 5 x 10(-3) at 25 degrees C, Fluid Phase Equilib. 207 (2003) 301–317.
[55] G. Scambia, P.B. Panici, G. Baiocchi, L. Perrone, S. Greggi, P. Di Roberto, S. Mancuso, CA 15-3 serum levels in ovarian cancer, Oncology 45 (1988) 263–267.
[56] S. Chourin, D. Georgescu, C. Gray, C. Guillemet, A. Loeb, C. Veyret, J.P. Basuyau, Value of CA 15-3 determination in the initial management of breast cancer patients, Ann. Oncol. 20 (2009) 962–964.